Cortical Networks for Control of Voluntary Arm Movements under Variable Force Conditions

Daniel Bullock, Paul Cisek and Stephen Grossberg

Department of Cognitive and Neural Systems, Boston University, Boston, MA, USA

A neural model of voluntary movement and proprioception is developed that offers an integrated interpretation of the functional roles of diverse cell types in movement-related areas of primate cortex. The model circuit maintains accurate proprioception while controlling voluntary reaches to spatial targets, exertion of force against obstacles, posture maintenance despite perturbations, compliance with an imposed movement, and static and inertial load compensations. Computer simulations show that properties of model elements correspond to the properties of many known cells types in areas 4 and 5. Among these properties are delay period activation, response profiles during movement, kinematic and kinetic sensitivities, and latency of activity onset. In particular, area 4 phasic and tonic cells, respectively, compute velocity and position commands that are capable of activating alpha and gamma motor neurons, thereby shifting the mechanical equilibrium point. Anterior area 5 cells compute the position of the limb using corollary discharges from area 4 and feedback from muscle spindles. Posterior area 5 neurons use the position perception signal and a target position signal to compute a desired movement vector. The cortical loop is closed by a volition-gated projection of this movement vector to the area 4 phasic cells. An auxiliary circuit allows phasic-tonic cells in area 4 to incorporate force command components needed to compensate for static and inertial loads. After reporting simulations of prior experimental results, predictions are made for both motor and parietal cell types under novel experimental protocols.

Introduction

Single-cell recording studies with alert primates trained to hold arm postures and perform voluntary arm movements have implicated the primary motor cortex (area 4) and parietal cortex (especially area 5) in a broad range of functions involving forelimb control and sensation. Among these are four linked functions of the voluntary movement system: (i) continuous trajectory formation; (ii) priming, gating and scaling of movement commands; (iii) static and inertial load compensation; and (iv) proprioception. Voluntary movement plans can be primed before some later decision to enact the movement, and voluntary trajectories can be slowed down and sped up, or halted in mid-course, at will. Activity interpretable as motor command priming has been observed in areas 5 and 4 (Crammond and Kalaska, 1989; Alexander and Crutcher, 1990; Riehle *et al.*, 1994), and continuous, scaleable and interruptible activities corresponding to evolving trajectory commands have been observed in area 4 (Evarts, 1973, Evarts, 1974; Evarts and Tanji, 1974; Georgopoulos *et al.*, 1982, 1984; Kettner *et al.*, 1988; Crutcher and Alexander, 1990; Burbaud *et al.*, 1991; Caminiti *et al.*, 1991; Scott and Kalaska, 1995). Voluntary forelimb activity in primates is specialized for transporting and manipulating a wide range of objects of diverse mass. Controlling such movements requires accurate proprioception despite load variations, as well as finely graded force generation, in order to compensate for both inertial and static loads associated with the manipulated objects. Activity interpretable as static and inertial load compensation has long been associated with area 4 (Evarts *et al.*, 1983; Kalaska and Hyde, 1985; Kalaska *et al.*, 1989; Crutcher and Alexander, 1990; Fetz, 1992), and a proprioceptive role for area 5 is also well established (Jennings *et al.*, 1983; Chapman *et al.*, 1984; Riehle *et al.*, 1994; Lacquaniti *et al.*, 1995).

Alert-animal recording studies have now produced a large inventory of physiologically identified cell types in areas 4 and 5. Connectivity tracing studies have also identified many of the afferent sources and efferent targets of pathways terminating in each area. However, hypotheses seeking to relate the implied global circuit structure to the physiological observations have been rare (Kalaska and Crammond, 1995; Kalaska, 1996), and there have been no hypotheses comprehensive enough to simultaneously relate the four functions mentioned above to the existing inventory of cell types and connectivities. This paper introduces such a set of hypotheses. The physiological and anatomical sources that were pivotal in formulating the hypotheses are given in Tables 1 and 2, which also give functional names for processing stages to be outlined below. On the basis of this data tabulation and computational constraints, we propose the model shown in Figure 1 and Table 1, as described below.

Methods

The model can be viewed as an extension and revision of the Vector-Integration-To-Endpoint, or VITE, model of Bullock and Grossberg (1988). The VITE model was addressed primarily to psychophysical data and provided neural interpretations for the variables DV, TPV, PPV and GO that are defined herein. It also treated proprioception differently, and did not analyze how area 4 assembles a multicomponent motor command that simultaneously specifies desired position and load-compensating forces.

The present model proposes that:

1. An arm movement difference vector (DV) is computed in parietal area 5 from a comparison of a target position vector (TPV) with a representation of current position called the perceived position vector (PPV). The DV command may be activated, or primed, prior to its overt performance.
2. The PPV is also computed in area 5, where it is derived by subtracting spindle-based feedback of position error, which is routed to area 5 via area 2, from an efference copy of an outflow position vector (OPV) from area 4.
3. The primed DV projects to a desired velocity vector (DVV) in area 4. A voluntarily scalable GO signal gates the DV input to the DVV in area 4. By virtue of the scaled gating signal, the phasic cell activity of the DVV serves as a volition-sensitive velocity command, which activates lower centers including gamma-dynamic motoneurons.
4. The DVV command is integrated by a tonic cell population in area 4, whose activity serves as an outflow position vector (OPV) to lower centers, including alpha and gamma-static motoneurons. This area 4 tonic cell pool serves as source of the efference copy signal used in

Cerebral Cortex Jan/Feb 1998;8:48–62; 1047–3211/98/$4.00

Table 1
Proposed correspondence between model elements and cell types

Model element	Cell type by physiology	References
Desired velocity vector (DVV)	area 4 phasic movement-time (MT)	Georgopoulos *et al.* (1982), Fromm *et al.* (1984), Kalaska *et al.* (1989)
Outflow position vector (OPV)	area 4 tonic	Fromm *et al.* (1984), Kettner *et al.* (1988), Kalaska *et al.* (1989)
Outflow force + position vector (OFPV)	area 4 phasic-tonic	Cheney and Fetz (1980, 1984), Fromm *et al.* (1984), Kalaska *et al.* (1989)
Inertial force vector (IFV)	area 4 phasic reaction-time (RT)	Kalaska *et al.* (1989)
Static force vector (SFV)	area 4 or subcortical?	unknown
Difference vector (DV)	posterior area 5 phasic	Chapman *et al.* (1984), Crammond and Kalaska (1989), Kalaska *et al.* (1990), Burbaud *et al.* (1991), Lacquaniti *et al.* (1995)
Perceived position vector (PPV)	anterior area 5 tonic	Kalaska and Hyde (1985), Kalaska *et al.* (1990), Burbaud *et al.* (1991), Lacquaniti *et al.* (1995)
Target position vector (TPV)	area 5 or area 7b	Robinson and Burton (1980), Anderson (1987), Dum and Strick (1990), Lacquaniti *et al.* (1995)
GO signal	globus pallidus	Horak and Anderson (1984a,,b), Kato and Kimura, (1992)

Table 2
Evidence for some of the connectivity assumed in the model

Model connection	Corresponding pathway	References
Spindle–SI	spindle to SI	Oscarsson and Rosen (1963), Phillips *et al.* (1971), Prud'homme and Kalaska (1994)
SI–PPV	SI to area 5	Jones *et al.* (1978)
OPV–PPV	area 4 to area 5	Pandya and Kuypers (1969), Evarts (1974), Jones *et al.* (1978), Brooks (1986)
PPV–OPV	anterior area 5 to area 4	Jones *et al.* (1978), Strick and Kim (1978), Zarzecki *et al.* (1978), Johnson *et al.* (1993)
DV–DVV	posterior area 5 to area 6	Jones *et al.* (1978)
	area 5 to area 4	Strick and Kim (1978), Zarzecki *et al.* (1978), Johnson *et al.* (1993)
OPV–gamma MNs	area 4 to gamma MNs	Pandya and Kuypers (1969), Brooks (1986)
OFPV–alpha MNs	area 4 to alpha MNs	Pandya and Kuypers (1969), Brooks (1986)

area 5 to compute the perceived position vector (PPV). As the movement evolves, the difference vector (DV) activity in area 5 is driven toward baseline. This leads to termination of excitatory input to area 4 phasic cells, and thus to termination of the movement itself.

5. A reciprocal connection from the area 5 PPV cells to the motor-cortical tonic cells (OPV) enables the area 4 position command to track any movement imposed by external forces. This reciprocal connection also helps to keep spindles loaded and to avoid instabilities that would otherwise be associated with lags due to finite signal conduction rates and loads.
6. Phasic-tonic force-and-position-related (OFPV) cells in area 4 enable graded force recruitment to compensate for static and inertial loads, using inputs to area 4 from cerebellum and a center that integrates spindle feedback. These area 4 phasic-tonic corticomotoneuronal cells enable force of a desired amount to be exerted against an obstacle without interfering with accurate proprioception (PPV), and while preserving a target posture (TPV) should the obstacle give way.

Testing this set of hypotheses against existing or future experimental data requires an understanding of the interactions of model mechanisms under various experimental conditions. Such implications can only be revealed by a simulation of a mathematically explicit model of the system. This section states computational properties of these hypotheses and describes how they were translated into a mathematical model. The Results section compares the output of model cells to recordings from distinct cell types in corresponding cortical areas under various experimental conditions.

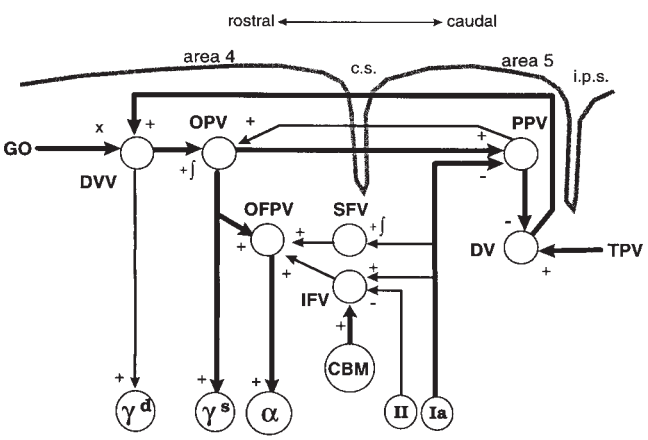

Figure 1 1. Cortical circuit model. Thick connections represent the kinematic feedback control aspect of the model, with thin connections representing additional compensatory circuitry. GO, scaleable gating signal; DVV, desired velocity vector; OPV, outflow position vector; OFPV, outflow force + position vector; SFV, static force vector; IFV, inertial force vector; CBM , assumed cerebello-cortical input to the IFV stage; PPV, perceived position vector; DV, difference vector; TPV, target position vector; γ^d, dynamic gamma motoneuron; γ^s, static gamma motoneuron; α, alpha motoneuron; Ia, type Ia afferent fiber; II, type II afferent fiber (position error feedback); c.s., central sulcus; i.p.s., intraparietal sulcus. The symbol + represents excitation, − represents inhibition, × represents multiplicative gating, and $+\int$ represents integration.

Continuous Trajectory Generation: Priming, Gating and Scaling of Movement Commands

To maintain focus on a more detailed treatment of neurophysiological data regarding temporal dynamics of cell types, the exposition is restricted to single-joint movements to specified target positions. The single-joint case is sufficient to address both kinematic and kinetic aspects of reaching, but has the virtue of avoiding the complexities of multi-joint coordination and spatial-to-motor transformations. Although the present discussion omits these complexities, the VITE trajectory generation circuit (Bullock and Grossberg, 1988) is capable of synchronizing movements among an arbitrary number of joints, as demonstrated elsewhere with multi-joint limbs (Bullock *et al.*, 1993) and more complex musculature involving mono- and bi-articular muscles (Contreras-Vidal *et al.*, 1997). The present discussion instead extends VITE to handle variable speeds and forces and shows that such an analysis permits the functional interpretation and simulation of properties of many types of identified cortical neurons.

The coordinate systems in which movements are planned and executed is not a central concern in this exposition. To avoid needless complexity, we treat the movement and posture commands as coded in muscle contraction coordinates. This simplification is empirically justified by data on precentral motor cortical cells studied in single and multi-joint movements (Evarts, 1968; Scott and Kalaska, 1995). However,

it is also made without loss of generality, because there are several known ways to embed muscle coordinate commands into more comprehensive neural architectures that learn to transform between spatial and motor coordinates (e.g. Bullock *et al.*, 1993). The core computational assumptions of the present model can be readily combined with alternative spatial and motor coding assumptions (Georgopoulos *et al.*, 1982; Mussa-Ivaldi, 1988; Caminiti *et al.*, 1991; Sanger, 1994; Scott and Kalaska, 1995).

To provide a physical setting for operation of the cortical circuits, it suffices to specify a minimal model of the sensory-motor periphery. Thus, let limb dynamics be described by

$$\frac{\mathrm{d}^2 p_i}{\mathrm{d}t^2} = \frac{1}{I}\left(M(c_i, p_i) - M\left(c_j, p_j\right) + E_i - V\frac{\mathrm{d}p_i}{\mathrm{d}t}\right) \tag{1}$$

where p_i is the contraction state, or position, of a muscle i within its range of origin-to-insertion distances, and $p_j = 1 - p_i$ is the position of the antagonist muscle j within its range. Indices i and j are used in this way throughout. Constraining the sum of p_i and p_j to equal 1 approximates the fact that lengthening either opposing muscle shortens the other. For simplicity, the position ranges from 0 to 1, with 1 the maximally compressed state of the muscle and 0 its maximally extended state. The parameter V is the joint viscosity and I is the limb's moment of inertia. External forces are represented by E_i, which is positive if the force assists shortening of the ith muscle and negative if it opposes.

The muscle function $M(\cdot)$ gives the force generated by a muscle given some contractile activity c_i and the position p_i. For simplicity, geometric effects due to moment arm, muscle yielding and non-linearities of force generation are ignored (see Bullock and Grossberg, 1991, for a discussion of these factors). The equation

$$M(c_i, p_i) = \left[L_i + M_i - \Gamma_i\right]^+ \tag{2}$$

depends on the length L_i of the muscle, the contraction level M_i and the muscle's resting length Γ_i. The threshold-linear function $[w]^+$ is defined as $\max(w,0)$. Defining $L_i = 1 - p_i$ and $\Gamma_i - M_i = 1 - c_i$ yields the muscle force function

$$M(c_i, p_i) = \left[c_i - p_i\right]^+ \tag{3}$$

The contraction activity c_i is governed by

$$\frac{\mathrm{d}c_i}{\mathrm{d}t} = v(-c_i + \alpha_i) \tag{4}$$

where α_i represents alpha motoneuron activity and υ scales the contraction rate.

The remainder of the system affects the limb by adjusting the alpha motoneuron activities. For voluntary movements, the system operates via area 4. The process of assembling the net descending command to alpha motoneurons can be divided conceptually into kinematic and kinetic aspects, of which the kinematic is treated first. The kinematic aspect of trajectory control involves specifying the time series of positions that the limb is intended to occupy between its initial and its desired final position. Kalaska *et al.* (1989) have classified movement-related cells in area 4 into major classes including tonic, phasic-tonic, phasic-MT (movement time) and phasic-RT (reaction time) cells, and compatible classifications have been discussed by others (Cheney and Fetz, 1980, 1984; Fromm *et al.*, 1984; Fetz, 1992). Tonic cells show static firing rates related to the position of the arm (Georgopoulos *et al.*, 1984; Kettner *et al.*, 1988; Caminiti *et al.*, 1991) and changes in activity related to the direction and extent of movement (Georgopoulos *et al.*, 1982; Kettner *et al.*, 1988; Riehle *et al.*, 1994). On the assumption that area 4 tonic cell activity through time codes a series of kinematic commands, it becomes necessary to ask how a cortical circuit generates input to be integrated by the area 4 tonic cells.

Area 4 phasic cells show changes in activity related to the direction (Georgopoulos *et al.*, 1982) and speed and/or amplitude of movement (Schwartz, 1992, 1993; Riehle *et al.*, 1994). The activities of phasic-MT cells decline over time as the movement progresses toward its endpoint (Kalaska *et al.*, 1989) and they are sensitive to both the direction and speed of movement (Schwartz, 1993). Direction (a vector) and speed (a scalar) together constitute velocity (a vector). The observations of Schwartz (1993) may be interpreted as evidence that such a vectorial velocity signal exists in area 4 (as opposed to merely a direction signal) and that it is coded in the activity of phasic-MT cells. The majority of these area 4 cells are non-primable and only respond during the actual movement (Evarts and Tanji, 1974) or immediately before. Finally, these cells show little sensitivity to the direction of load (Kalaska *et al.*, 1989). We therefore suggest that the non-primable, direction-specific and speed-sensitive phasic-MT cells in area 4 correspond to a representation of desired movement velocity and that the tonic cells integrate the phasic-MT activity. We thus treat both cell types as parts of a distributed kinematic trajectory generator capable of independently controlling the direction and speed of movement, as described below (see equation 13).

The tonic cell activity can be described by

$$\frac{\mathrm{d}y_i}{\mathrm{d}t} = (1 - y)\left[u_i - u_j\right]^+ - y_i\left[u_j - u_i\right]^+ \tag{5}$$

where y_i is the average firing rate of a population of area 4 tonic cells (the OPV), and u_i is the phasic-MT cell activity (the DVV). Equation (5) specifies that the tonic cell population will integrate its inputs. Activation increments and decrements depend on the difference between the agonist (u_i) and antagonist (u_j) phasic-MT activities. Activity ranges between 0 and 1, and $y_i + y_j = 1$. This constraint on the sum of tonic cell activities does not imply a constraint on the sum of alpha motoneuron activities, as clarified below in equation (18).

The phasic-MT (DVV) activity in area 4 is interpreted to be a gated and scaled version of a movement command that is continuously computed in area 5 as the vector difference (DV) between the target and the perceived limb position vectors. Area 5 DV cell activity can be described by

$$r_i = \left[T_i - x_i + B^{(r)}\right]^+ \tag{6}$$

where r_i is the activity of a DV cell, and $B^{(r)}$ is its baseline activity. The target position is expressed as T_i and current limb position (PPV) as x_i. These model area 5 cells fire at the baseline rate except when current and targeted limb position differ, i.e. during movement and movement priming intervals.

We identify the DV with phasic cells in posterior area 5 because the activities of such area 5 cells show no load sensitivity (Kalaska and Hyde, 1985; Kalaska *et al.*, 1990), decay gradually as the target is approached (Kalaska *et al.*, 1990), and can be 'primed' by the presentation of the target signal (Crammond and Kalaska, 1989) before the experimenter's 'go' stimulus. Such phasic cells in area 5 were also reported by Lacquaniti *et al.* (1995), who explicitly stated that this neuron class could be 'defined as "variational", related to the difference vector between final and initial position' (p. 403). Consistent with the reports from Kalaska's laboratory, Lacquaniti *et al.* (1995) reported that for such cells, RT activity was tuned in the same manner as MT activity.

Several equations describe computation of perceived position because it depends on both central commands and feedback from muscle receptors. (Visual feedback is not treated here.) These equations describe the computation of a PPV by anterior area 5 tonic cells that are assumed to receive an efference copy input from area 4 and position error feedback from muscle spindles:

$$\gamma_i^{\mathrm{S}} = y_i \tag{7}$$

$$\gamma_i^{\mathrm{D}} = \rho\left[u_i - u_j\right]^+ \tag{8}$$

$$s_i^{(1)} = S\left(\theta\left[\gamma_i^{\mathrm{S}} - p_i\right]^+ + \phi\left[\gamma_i^{\mathrm{D}} - \frac{\mathrm{d}p_i}{\mathrm{d}t}\right]^+\right) \tag{9}$$

$$s_i^{(2)} = S\left(\theta\left[\gamma_i^{\mathrm{S}} - p_i\right]^+\right) \tag{10}$$

$$S(w) = \frac{w}{1+100w^2} \tag{11}$$

$$\frac{dx_i}{dt} = (1-x_i)\left[\Theta y_i + s_j^{(1)}(t-\tau) - s_i^{(1)}(t-\tau)\right]^+ - x_i\left[\Theta y_j + s_i^{(1)}(t-\tau) - s_j^{(1)}(t-\tau)\right]^+ \tag{12}$$

where γ_i^S is the activity of static gamma motoneurons, γ_i^D is the activity of dynamic gamma motoneurons, $s_i^{(1)}$ is the activity of primary spindle afferents from muscle i, $s_i^{(2)}$ is the activity of secondary afferents, the function $S(\cdot)$ describes spindle saturation, ρ is a scaling parameter, θ is the sensitivity of static nuclear bag and chain fibers, ϕ is the sensitivity of the dynamic nuclear bag fibers, x_i is the average firing rate over a population of anterior area 5 tonic cells (PPV), and Θ is the gain of the corollary discharges from area 4 tonic cells, calibrated such that $\Theta \approx \theta$, to ensure accurate PPV calculation. The variable t indicates the time index and τ the delay in feedback to central sites. Because $y_j = 1 - y_i$ and $p_j = 1 - p_i$, equation (12) implies that x_i approximately tracks position p_i at rate θ.

The use of spindle signals as the primary source of peripheral feedback on limb position is consistent with psychophysical evidence that spindles underlie position sense (Goodwin *et al.*, 1972; Clark *et al.*, 1979). This is not, however, meant to equate the PPV representation with the conscious perception of position, which presumably requires additional neural mechanisms. The fact that anaesthetized subjects are able to perform movements without being aware of this (Goodwin *et al.*, 1972) suggests that, while the PPV may be sufficient to control the movement, it is not sufficient to bring the movement to the subject's conscious awareness.

We identify the model's computation of current limb position with tonic cells in anterior area 5 because such cells show activities that vary with limb position (Kalaska *et al.*, 1990) and have very little load sensitivity (Kalaska and Hyde, 1985; Kalaska *et al.*, 1990). Anterior area 5 receives projections from area 4 and from spindle-receiving somatosensory areas (Oscarsson and Rosen, 1963; Phillips *et al.*, 1971; Jones *et al.*, 1978), where cell activities correlate with position error (Fromm and Evarts, 1982). Target representations may exist in posterior area 5 (Lacquaniti *et al.*, 1995) and/or in more caudal regions of parietal cortex such as area 7b (Robinson and Burton, 1980; Anderson, 1987; Dum and Strick, 1990).

If the limb always obeyed the position command (OPV), then limb position could be computed by using only an efference copy of the descending command from area 4 tonic cells. Under most realistic conditions, however, the estimate based on the commanded position needs to be corrected using a feedback-based error signal. Such a signal is available from muscle spindles (Vallbo, 1981), which have been shown to be the primary non-visual sensory source of information on limb position (Goodwin *et al.*, 1972; Clark *et al.*, 1979; Matthews, 1988; McCloskey *et al.*, 1983).

Figure 2 illustrates how spindles can be used to compute a positional error. Spindles have long been recognized to respond sensitively to small but not large stretches, and it has been argued (Kuffler and Hunt, 1952) that the intrafusal contraction serves to maintain spindle sensitivity by resetting the base length relative to which the spindle can sensitively register the degree (or rate) of stretch. This is equivalent to saying that, to maintain sensitivity, the intrafusal length is set to the expected length of the extrafusal, in which case an above-baseline spindle firing rate will indicate a positive length discrepancy of the extrafusal ('stretch') and a below-baseline spindle discharge rate will indicate a negative length discrepancy of the extrafusal muscle ('excess contraction'). During voluntary movement, if the intrafusal length is continuously updated to reflect the desired extrafusal length, then the measured length discrepancies can serve as a signed error feedback to the neural controller. If a load retards movement unexpectedly, then the spindle response may saturate in the agonist and fall silent in the antagonist, but the sign of the error feedback will remain accurate.

System (1)–(12) describes a central trajectory generator and the single joint it controls by a pair of antagonistic muscles, with one critical gap: the gating operation, or GO signal, that transforms the primable DV activity in area 5 into scaled DVV (area 4 phasic-MT cell) activity. The model proposes that this gating operation is what allows parietal

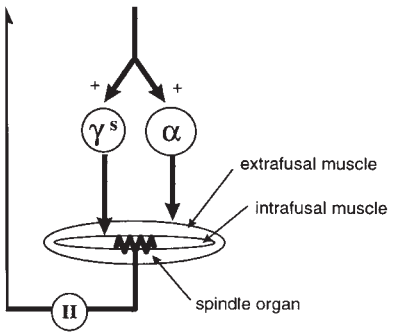

Figure 2. Spindle computation of positional error. Alpha- and gamma-static motoneurons receive a desired contraction command. If the extrafusal muscle is kept from contracting, then the spindle organ is stretched by the contraction of the intrafusal muscle and secondary spindle afferents report a position error.

targeting to actually gain control of the frontal effector apparatus. It can be represented mathematically by

$$u_i = \left[g \cdot (r_i - r_j) + B^{(u)}\right]^+ \tag{13}$$

where u_i is the area 4 phasic MT cell activity (DVV), r_i is the DV, g is the GO signal, and $B^{(u)}$ is the baseline activity for the DVV.

Because the model DVV stage computes a product of the DV and the GO signal, our interpretation implies that the corresponding cell type, area 4 phasic-MT cells, should be sensitive to both the speed of movement and to movement extent. The former sensitivity was reported by Schwartz (1993; see also Georgopoulos, 1995) and the latter by Fu *et al.* (1993). Moreover the multiplicative action of the GO signal implies that it controls the magnitude of the phasic-MT vector without altering its direction, and thus can be used to scale the speed of movement. When the target is presented before the experimenter's 'go' stimulus is given, the posterior area 5 difference vector activates, but withholding or inhibiting the internal GO signal prevents activation of area 4 phasic-MT cells. Inhibition of an active GO signal can also be used to rapidly abort movement. For these reasons we regard the basal ganglia, whose degeneration in Parkinson's disease results in slowed movement, mid-movement freezing and difficulty in initiating movement, as a strong candidate for control of gating, which could operate via the fronto-striato-pallido-thalamic pathway to area 4 (Bullock and Grossberg, 1991).

The GO signal is assumed not to turn on abruptly, but rather to grow as a sigmoidal function of time. For simplicity, equations for a two-step cellular cascade were used to generate the sigmoidal GO signal:

$$\frac{dg^{(1)}}{dt} = \varepsilon\left(-g^{(1)} + \left(C - g^{(1)}\right)g^{(0)}\right)$$

$$\frac{dg^{(2)}}{dt} = \varepsilon\left(-g^{(2)} + \left(C - g^{(2)}\right)g^{(1)}\right)$$

$$g = g^{(0)}\frac{g^{(2)}}{C} \tag{14}$$

where g is the GO signal that multiplies the DV (see equation above), $g^{(0)}$ is the step input from a forebrain decision center, ε is a slow integration rate, and C is the value at which the GO cells saturate. Any cascade larger than 2 will also generate a sigmoidal GO signal. An analysis of GO signal shape and its effect on the bell-shaped velocity profile observed during movements can be found in prior reports (Bullock and Grossberg, 1988).

The hypothesis that area 4 phasic-MT cell activity constitutes a volition-gated difference vector predicts that these cells will exhibit preferred-direction tuning during active movement, and will show enhanced response if a perturbation temporarily moves the arm in a direction opposite to their preferred direction (since this increases the difference between current position and the target). This model cell

property is in agreement with data on area 4 phasic-MT cells reported in Evarts and Tanji (1974).

Proprioception, Compliance with Imposed Movement, and Load Compensation

In system (1)–(14), a relaxed state can be specified by setting the GO signal to zero, thereby shutting down new inputs to the integration operation performed by area 4 tonic cells. The joint will hold the position last specified, and any externally imposed movement will cause a buildup of tension in the muscles antagonist to the external force. If the external force is released, the joint will spring back to the internally specified position. In all, the limb will trace a U-shaped trajectory.

Although characteristic of equilibrium point models and useful as one mode of system operation, such behavior is insufficient to willfully comply with an imposed movement. In that mode, the limb is relaxed as movement is imposed by an external force, tension does not build up, and when the external force disappears, the actor can hold the limb in the new, externally imposed position. In the model, this requires updating of the OPV during the passive movement. Updating is accomplished through a projection from the anterior area 5 position cells (PPV) to the area 4 tonic cells (OPV), as shown in Figure 1. In the absence of phasic-MT activity (which mediates willful resistance), this projection causes the position specified by the tonic cells to track the perceived position vector (see equation 15 below). This mechanism not only allows tension to be released in the relaxed state, but keeps spindles loaded and thus ensures that the system remains sensitive to limb position. The bidirectional projection between tonic cells in areas 4 and 5 also adds significant stability to the system (see Fig. 11 below).

With the addition of the reciprocal area 5 to area 4 pathway, equation (5) for the area 4 tonic cell (OPV) activity is augmented as

$$\frac{dy_i}{dt} = (1 - y_i)\left(\eta x_i + \left[u_i - u_j\right]^+\right) - y_i\left(\eta x_j + \left[u_j - u_i\right]^+\right) \qquad (15)$$

where η is the gain of the projection from anterior area 5 (PPV) to area 4 tonic cells (OPV).

The U-shaped trajectory discussed above is observed when the limb of a deafferented (vision-blocked and dorsal-rhizotomized) monkey is surreptitiously moved by the experimenter to the vicinity of a target and released simultaneously with the 'go' stimulus to perform a voluntary movement to that same target (Bizzi *et al.*, 1984). The model is consistent with this observation since, in the absence of spindle feedback, the OPV remains at the initial target position during the imposed displacement, tension builds up, and the arm springs back towards the initial position before turning toward the target as the OPV is updated by integration of the DVV. This property is simulated below (see Fig. 6).

In the circuit described by (1)–(15), if an obstacle prevents movement, then spindle feedback (Ia in Fig. 1) will notify the system that the arm has stopped moving and thus the area 5 difference vector will not fully return to baseline. If the GO signal remains on, then integration by area 4 tonic cells will continue, effectively shifting the equilibrium point of the limb, but not the limb itself, past the obstacle. Because of the spring property of muscle, the force exerted against the surface will grow as long as the GO signal remains on or until the force production limit of the system is reached. If the obstacle yields, the equilibrium point, and the limb, will move to the location specified by the target position vector.

Within system (1)–(15), inertial effects can cause the limb's trajectory to show sizable transient mismatches with the trajectory specified by the evolving OPV. The limb will lag the OPV at the beginning of movement, and overshoot the target briefly at the end. Such undesirable effects can be partly compensated by circuitry that reduces velocity errors. In the model, this compensation is achieved if the projection from area 4 to spinal motoneurons is split into two parallel pathways, one to the alpha motoneurons (α in Fig. 1) and one to the static gamma motoneurons (γ^s in Fig. 1). Interposed along the pathway from area 4 tonic cells to alpha motoneurons is a population of cells (OFPV in Fig. 1) that receives a compensatory launching pulse in addition to the tonic cell command. The launching pulse helps overcome the inertia of the limb at the beginning of movement. We identify the interposed model cell population with area 4 phasic-tonic cells (Kalaska *et al.*, 1989), whose activity profile is interpretable as a superposition of a launching pulse and a tonic signal related to the shifting OPV. That these OFPV cells are motor-cortical output cells corresponds to the observation by Cheney and Fetz (1980) that 59% of cortico-motoneuronal projection neurons are of the phasic-tonic type.

The launching pulse itself we identify with activity of phasic reaction-time (RT) cells (Kalaska *et al.*, 1989). In the simplest scheme, this pulse, whose purpose is to cause an acceleration to compensate for inertia, can be based on a velocity error signal. Such a signal is available in the feedback from primary spindle afferents (Vallbo, 1981) (Ia in Fig. 1), and it becomes available in the model if the dynamic gamma motoneurons (γ^d in Fig. 1) receive a signal proportional to desired velocity. Dynamic gamma motoneurons are modeled as recipients of the DVV signal that is derived from area 4 phasic MT cells, and thus they provide a velocity reference for computation of velocity error, analogous to the position reference provided by static gamma motoneurons.

The activity of the phasic RT cells, which constitutes an inertial force vector (IFV), is governed by

$$q_i = \lambda_i\left[s_i^{(1)}(t-\tau) - s_i^{(2)}(t-\tau) - \Lambda\right]^+ \qquad (16)$$

where λ_i is the feedback gain and Λ is a threshold. This activity is added to the signal from the area 4 tonic cells to produce phasic-tonic activity, which constitutes an outflow force + position vector (OFPV)

$$a_i = y_i + q_i \qquad (17)$$

which then projects to the alpha motoneurons

$$\alpha_i = a_i + \delta s_i^{(1)} \qquad (18)$$

where δ is the gain of the stretch reflex. Because of the convergence of various sources of input on the alpha motoneuron activities, the sum of these activities is not constrained to be constant as is the sum of OPV activities and the sum of muscle lengths. Though not pursued here, the model can thus incorporate additional excitatory inputs to alpha motoneurons, such as those used (Humphrey and Reed, 1983) to co-contract opposing muscles and stiffen a joint without altering joint angle (Bullock and Grossberg, 1989, 1990).

Available theory and data indicate that it is possible to pre-empt inertia-induced and other errors generated during well-rehearsed movements by making use of the adaptive cerebellar side-loop (Vilis and Hore, 1980; Ito, 1984; Bullock and Grossberg, 1991; Kawato and Gomi, 1992; Fiala *et al.*, 1996; Contreras-Vidal *et al.*, 1997). If the cerebellum learns to predict velocity errors based on movement context, it can automatically generate appropriate launching pulses in area 4 before errors occur. Such a feedforward compensation circuit avoids oscillations due to feedback delays, and can operate at a much higher gain than a feedback circuit. In some simulations below, we approximate the pre-emptive function of such a cerebellar feedforward side-loop by reducing the delay (τ) on spindle feedback to zero. This is not meant to imply a non-physiological zero-delay in feedback, but is merely a way to mimic the availability of a calibrated feedforward compensation. [See Bullock and Grossberg (1991) and Contreras-Vidal, *et al.* (1997) for further discussion.] If we did not assume feedforward anticipatory compensation (i.e. if the feedback delay were increased), then during fast movements the model would exhibit oscillations, which are indeed observed during cerebellar cooling (Vilis and Hore, 1980).

System (1)–(18) is able to deal with obstacles that act to constrain position but do not themselves exert a constant force. The motor system is also able to accurately respond to static loads during voluntary movement and posture. Gravity, for example, is a constant load that pulls the limb out of any non-vertical target configuration. Even with a positive GO signal, system (1)–(18) cannot completely compensate for such loads, and the limb will equilibrate at a position displaced from the target. This property motivates the introduction of a static load compensation mechanism.

A simple way to resist perturbation by loads is to increase the stiffness of the joint through strong co-contractions. Co-contraction cells (cells that are sensitive to movement but are not direction selective) and muscle co-contractions are indeed observed *in vivo* (Humphrey and Reed, 1983)

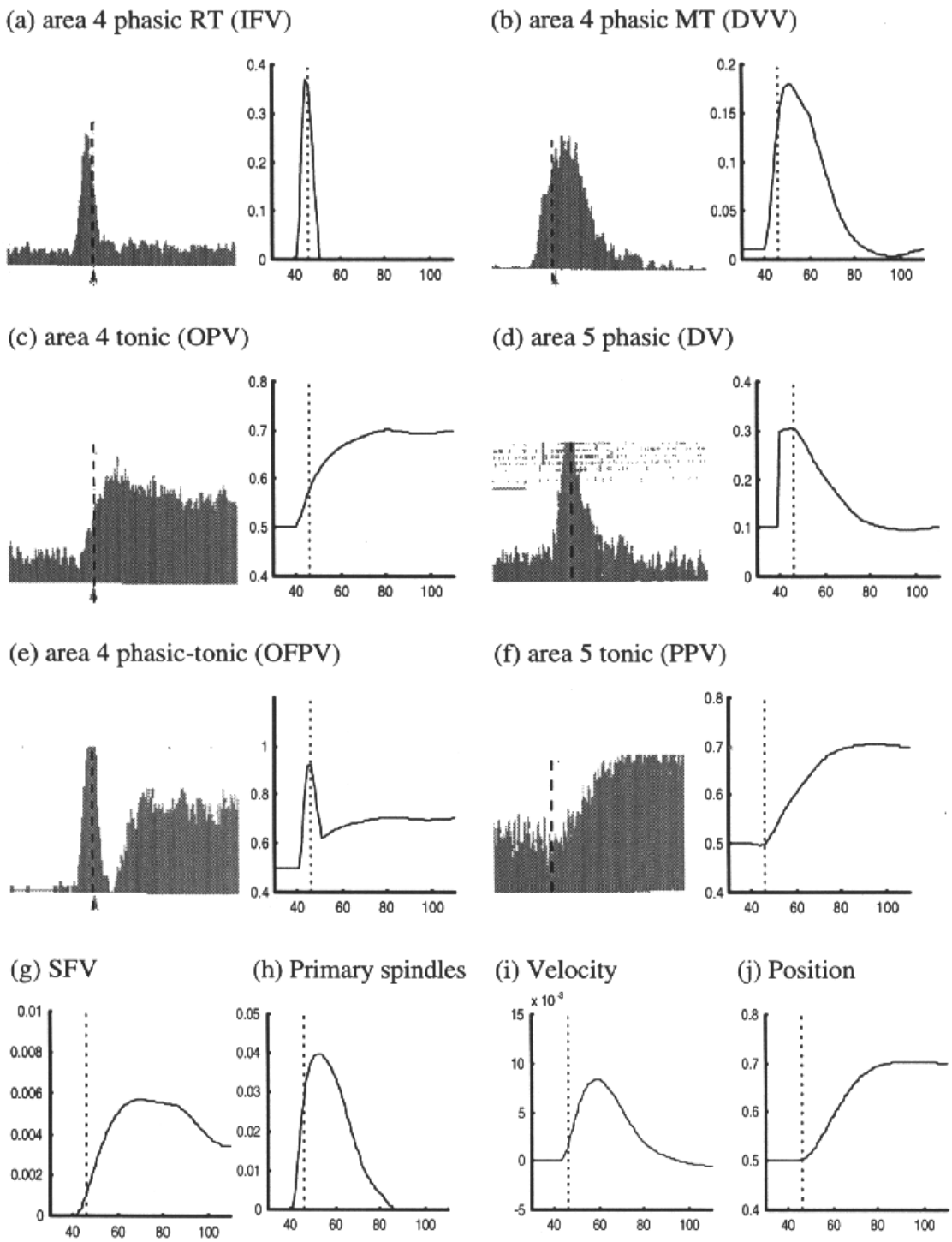

Figure 3. Comparison of cortical activity and model cell responses during a simple voluntary reaching task. Histograms in (*a*)–(*c*) and (*e*) are taken from Kalaska *et al.* (1989) and (*d*) and (*f*) are from Kalaska *et al.* (1990). Histograms are centered on the onset of movement, which is indicated in both the data and the simulations by a vertical dashed line. This can be used to compare the relative onset times in the different neural cell types and model elements. (*g*) Simulation of the SFV population. (*h*) Simulation of primary spindle activities during movement. (*i*, *j*) Velocity and position traces. In the simulations presented above, a GO signal of $g^{(0)} = 0.75$ was used and pre-emptive feedforward compensation approximated by reducing $\tau = 0$ and increasing $\lambda_1 = 150$. For reasons given in the text, this is not meant to imply a non-physiological zero-delay *in vivo*. In this and subsequent simulations, 1 s of time is ~100 time steps.

when the direction of action of a static load is unpredictable or changes too rapidly for voluntary compensation. Prior modeling work (Bullock and Grossberg, 1989, 1990; Bullock and Contreras-Vidal, 1993) indicates how stiffness control can operate without disrupting position control and proprioception. However, co-contractions increase the limb's resistance to movement in all directions, thereby interfering with voluntary movements. They are also insufficient for full compensation, and are energetically inefficient.

An efficient static load compensation circuit should generate a canceling force only in the direction opposing the load. One alternative is to reduce the gain in the pathway from the anterior area 5 tonic cells (PPV) to the area 4 tonic cells (OPV). This would enable the OPV cells to continue integrating until the DV has been completely reduced to zero. However, reducing the gain of the area 5 to area 4 signal would reduce the stabilizing influence of this pathway and lead to significant overshoots and endpoint oscillations (see Fig. 11).

The alternative incorporated in the model operates by integrating over time the position error feedback from the spindles. This generates a static force vector (SFV) which is added to the activity of area 4 phasic-tonic cells (OFPV). This compensating signal is added to the phasic-tonic cells rather than to the tonic cells of area 4 in order to preserve the status of the tonic cells' command to static gamma motoneurons as a purely kinematic reference signal, corresponding to the desired extrafusal length, for the spindle subsystem. Because the integrated value of the SFV continues to change until the spindle signal (and position error) reaches zero (or, equivalently, becomes equal in antagonist and agonist channels), linear calibration is not necessary, as long as the bias is zero and the gain is not too high. Also, because an increase in alpha motoneuron activity can only reduce spindle output, the spindle pathway to the SFV closes a *negative* feedback loop. This circuit is similar to the stretch reflex, but the interposed integration process allows operation at a somewhat higher gain without causing oscillations, because integration filters out high-frequency components of an incoming signal.

The following equation describes the behavior of the SFV population:

$$\frac{df_i}{dt} = (1 - f_i)hs_i^{(1)}(t-\tau) - \psi f_i\left(f_j + s_j^{(1)}(t-\tau)\right) \qquad (19)$$

where h is a gain that controls the strength and speed of load compensation, and ψ is a parameter scaling inhibition by the antagonist component of the SFV and by the antagonist spindle. The SFV signal is an added input to the phasic-tonic cells (OFPV), so equation (17) is replaced by

$$a_i = y_i + q_i + f_i \qquad (20)$$

A distinct *in vivo* cell type corresponding to model SFV cells has not, to date, been identified. If such cells exist in area 4, they would be lumped together into the 'tonic' group, since their activities are primarily tonic and they would often show modest movement-related modulation and load-related responses. An SFV integrator might also be located subcortically.

Results

This section reports simulation results that compare identified cortical cells with model cells. It is divided into three parts. The first part reports simulations which show that trajectories of model variables match observed trajectories of corresponding brain variables in a range of experimental tasks. Because observations of corresponding brain variables are not known for the full set of model variables in each task, each simulation also makes testable predictions. The second part reports simulations which predict how measurable brain variables should behave in new experimental tasks if the model is correct. All the simulations in both parts are based on equations (1)–(4), (6)–(16), (18)–(20) and on the parameters listed in the Appendix, unless otherwise noted. The third part discusses how the model compares with control theory concepts.

Simulations of Prior Experimental Tasks

Basic Point-to-point Movement: Synchronous Activation of the Target and Go Stimuli

The simplest type of point-to-point movement task is one in which the animal holds its hand at a prescribed initial point, and then moves its hand without an imposed delay to the position of a target light when that light turns on. The light-on event is thus both a target specification and a 'go' stimulus. As shown in Figure 3*j*, the model is capable of performing such movements accurately, sometimes exhibiting transient overshoots (Lestienne, 1979; Gachoud *et al.*, 1983), but always reaching the target as long as the GO signal remains positive. The smooth, bell-like shape of the velocity profile is largely a function of the central aspects of the circuit, e.g. gradual onset of the GO signal, but is also aided by such factors as the saturation of the spindle feedback signal as trajectory errors become very large. Figure 3 also evaluates the model's ability to simulate observations made on cortical cells of monkeys performing this task. For each model cell type for which a cortical correspondent was proposed, a representative histogram is shown from an experimental report of single cell activities in monkeys during performance of this task, along with an activity–time plot of the corresponding model cell type. The modeled and real cell types exhibit qualitatively similar activation trajectories.

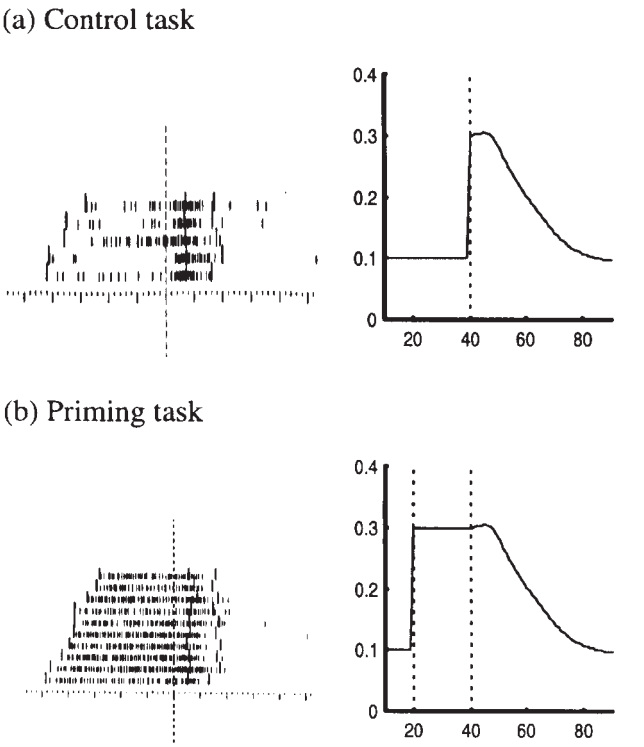

Figure 4. Comparison of model DV and area 5 phasic activity during a control task (*a*) and a priming task (*b*), where the target is shown before the 'go' stimulus is given. The times of the target presentation and the 'go' stimulus are shown as a vertical dashed line. This simulation used the same parameters as that of Figure 3. Rasters reprinted from Crammond and Kalaska (1989).

Figure 3 compares our single-joint model with data collected during two-dimensional movements. We believe this comparison to be valid. The data sets from single- and multi-joint studies both reflect the same computational issues. Further modeling studies that use multiple joints and large neural populations could nonetheless offer a more detailed account of these data. For example, by using a distributed population of OFPV neurons with a gradient of thresholds for tonic activation, one could simulate the brief period of silence (not present in the current OFPV simulation; Fig. 3*e*) that is sometimes observed to follow the initial phasic burst of the phasic-tonic cell (Kalaska *et al.*, 1990). More generally, the model is compatible with a wide distribution of time lags between the phasic and tonic

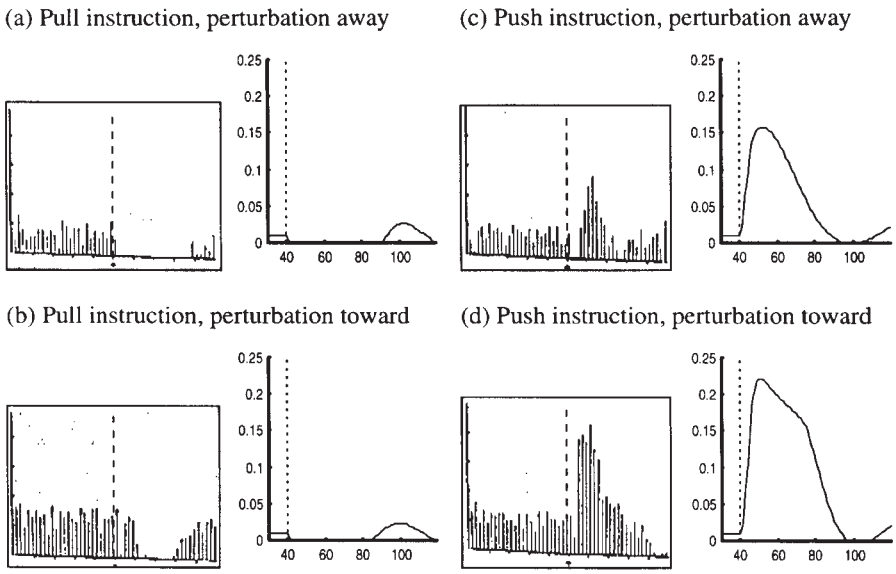

Figure 5. Simulation of Evarts and Tanji's (1974) paradigm. Vertical line indicates the time of the perturbation. In the simulations, a GO signal of $g^{(0)} = 0.8$ was used.

components of OFPV-type phasic-tonic cells, because changes in the OPV-correlated and SFV-correlated parts of the tonic component need not have the same sign, time course or amplitude. Thus one part can mask the other for intervals that are strongly dependent on limb-geometry, dynamic postural demands of the task, load-direction, etc.

The model is also consistent with observations on the relative onset latency of these cells. For example, during voluntary movement, Burbaud *et al.* (1991) have shown the following sequence of onsets: Posterior area 5 cells activate first, before movement starts. Shortly afterwards activities change in area 4. Area 2 cells activate during movement, and finally anterior area 5 cells activate after movement has begun. The model onset latencies are similar: DV cells corresponding to posterior area 5 activate first, followed by DVV and OPV cells in area 4. These events are followed by movement and by activities in PPV cells in anterior area 5. If area 2 cells code positional error, as suggested by Fromm and Evarts (1982), then one would expect them to exhibit activity during movement.

Point-to-point Movement with Priming: Go Stimulus Onset Lags Target Stimulus Onset

In a priming task, the target location is specified earlier than the time of 'go' stimulus onset, so it is possible for the animal to pre-activate or prime a representation of the dimensions of the forthcoming movement. In the model, this occurs at the DV stage in area 5 at the time of the target presentation. Because the DV is not allowed to update the area 4 tonic cells (OPV), and thereby to erase itself, until the delayed 'go' stimulus activates the internal GO command, the model is consistent with the observation that area 5 activity begins at the time of target presentation and persists at full strength until after the 'go' stimulus is given. Figure 4 shows representative rasters for an area 5 phasic cell in a priming task and a control task. Alongside of these are shown simulations of model DV activity. In the priming task, both the real and model cells activate and hold steady at a high level until after the 'go' stimulus is given, at which time the DV begins to return toward baseline.

Point-to-point Movement with Limb Perturbation as the Go Stimulus

In this task (Evarts and Tanji, 1974), the experimenter delivers the 'go' stimulus in the form of a perturbation to the limb that is about to perform the task of pushing or pulling a lever to a target position. In the model, the perturbation has two separate direct effects: it activates the internal GO command, and it changes the internal representation of joint position (PPV). The change in joint position in turn affects the DV and, because of the active GO command, the DVV. Figure 5 allows comparison of the activity of an area 4 phasic-MT cell tuned to the direction of the push with the activity of a similarly tuned model DVV cell, for four conditions formed by crossing two targets (one reached by pulling the lever toward the monkey's body, one by pushing the lever away) with two directions of perturbation (one that moved the lever away from the monkey, and one that moved it nearer the monkey). The model fits the observed rank ordering of activation levels, which increase with the signed amplitude of the resultant DV.

U-shaped Movement after Deafferentation and Temporary External Fixation of the Limb at the Target Position

In this paradigm (Bizzi *et al.*, 1984), a monkey is trained to make single-joint movements to target lights from a prescribed, actively maintained, initial posture, and then deafferented by the combination of a permanent dorsal rhizotomy and temporary visual occlusion. Such monkeys remain capable of performing the task. This is expected from the model because the internal efference copy feedback is sufficient to allow target-distance scaled, self-terminating movements (albeit of reduced accuracy) after the corrective spindle feedback is removed. If under this condition the animal's arm is surreptitiously moved from the prescribed initial posture to the position of a target light before it is turned on, then the absence of the spindle to PPV pathway will prevent PPV updating and thus also adjustment of the OPV. Thus tension will build in the muscle opposing the experimenter's surreptitious displacement. If the experimenter then releases the arm and turns on the target light simultaneously, the arm will initially spring back toward the prescribed initial posture. However, because the target onset activates the internal

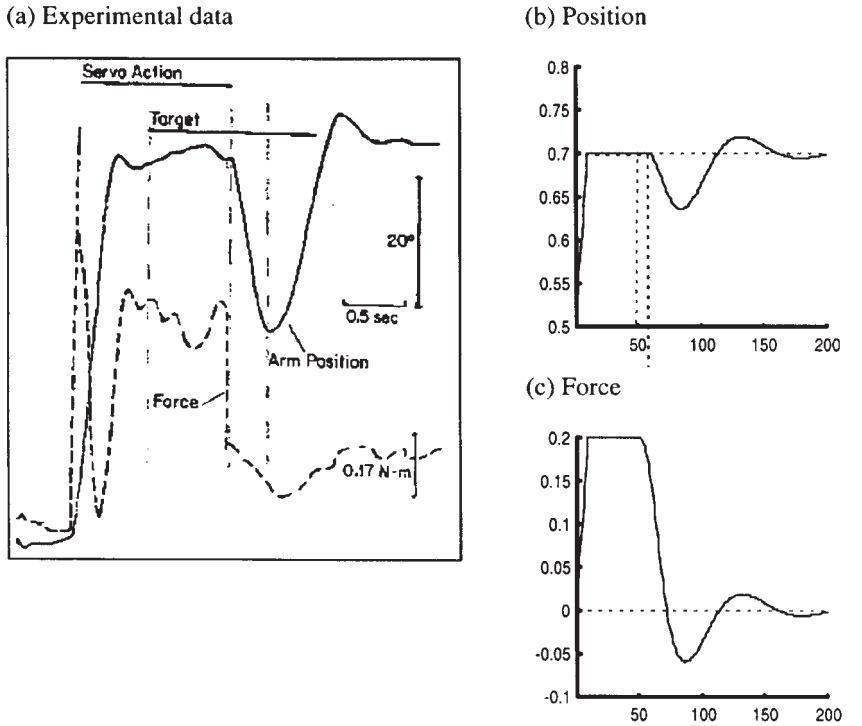

Figure 6. Simulation of movement with deafferentation and temporary external fixation of the limb at the target location. (*a*) Data from Bizzi *et al.* (1984) The servo moves the limb toward the target position, then when the servo turns off, the 'go' stimulus is given. (*b*) Position trace from the simulation. The dotted lines indicate the target location and the constraining action of the servo. The GO signal ($g^{(0)} = 0.5$) turns on when the target is given. (*c*) Force trace, calculated as $M(c_2,p_2) - M(c_1,p_1)$. Deafferentation was simulated by setting $\theta = \phi = 0$.

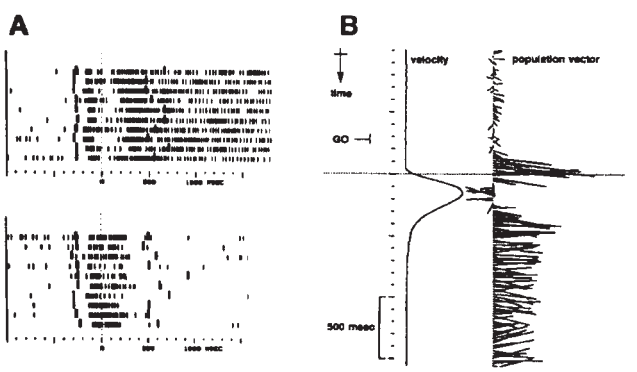

Figure 7. Population vector computed with contributions of phasic-tonic cells only. Reprinted from Kalaska and Drew (1993). (*a*) Rasters from phasic-tonic cells tuned to the direction of movement (top) and to the opposite direction (bottom). (*b*) Velocity trace and instantaneous population vector of 73 phasic-tonic cells during movement to the right. Movement onset is indicated by the horizontal line.

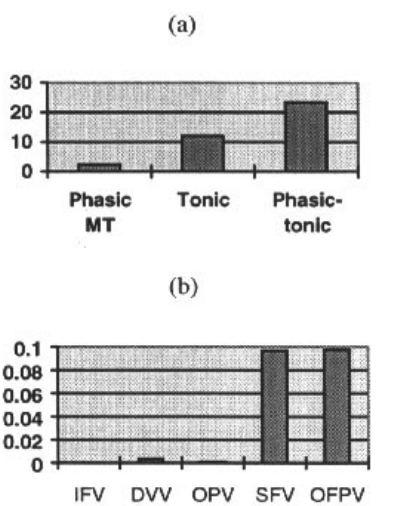

Figure 8. Comparison of load sensitivity in the data (*a*) (plotting the gain of the cosine tuning) and in the model (*b*) (plotting the difference in activation between a loaded and unloaded condition). See text for details.

trajectory generator, the DVV will begin to update the OPV (and PPV) in the direction of the target. Thus the arm's motion toward the initial posture will be arrested, and the arm will reverse direction and move toward the target. The resultant trajectory is U-shaped. This paradigm can be simulated with the model following elimination of the spindle feedback terms. Figure 6 shows that the model's output is comparable to an experimental arm trajectory obtained with this paradigm.

Point-to-point Movement with an Inertial Load

Under the assumption of prior learning by a feedforward IFV pathway, the model predicts that both launching and braking pulses should be apparent in the activity of the phasic-RT and phasic-tonic cells. Figure 7 reprints results from one of the few population vector analyses restricted to an identifiable cell type in area 4 (Kalaska and Drew, 1993). As can be seen, there is evidence for a launching pulse, a braking pulse and finally a tonic activation among the phasic-tonic cells. Though the model is consistent with these data, a population simulation needed for a direct comparison would require 'unlumping' of the model

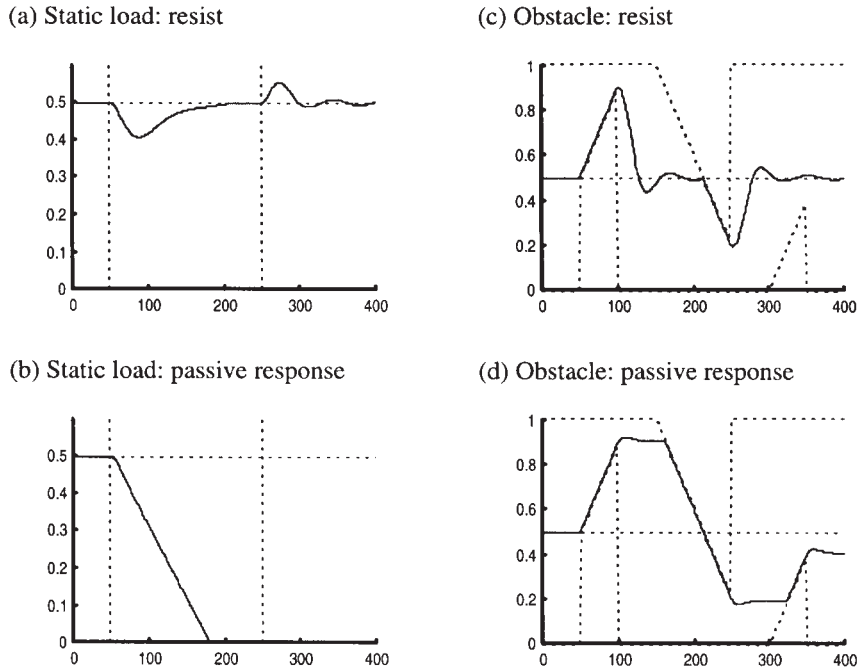

Figure 9. Active and passive responses to external perturbations. Solid lines indicate the position of the limb (with flexion positive). (*a*,*b*) Responses to a static load of $E_1 = 0.1$. Dashed vertical lines indicate onset and offset of the load. (*c*,*d*) Responses to obstacles. Dashed lines indicate the position-constraining action of the obstacles. Active resistance (*a*,*c*) is simulated by setting $g^{(0)} = 0.5$ and $h = 0.05$. Passive response (*b*,*d*) is simulated by setting $g^{(0)} = 0$ and $h = 0$. Target location is indicated by the horizontal dashed line.

elements and more careful consideration of distributed motor representations. Because these issues would complicate the model considerably, such a simulation is beyond the scope of this report.

Point-to-point Movement with a Static Load

A number of experiments have examined the static load sensitivity of several of the cortical cell types encompassed by the model. In this paradigm, a static load is imposed at the beginning of movement and it acts in a constant direction through the MT and into the target holding time (THT) that follows movement. In Figure 8, the load sensitivity of model elements is compared with the load sensitivity of cortical cells. Because the model reproduces single-joint movement only, the comparison is qualitative. Thus, to rank the load-sensitivity of cortical cells we follow Kalaska *et al.* (1989) and use the c_1 parameter from the equation $y = b_0 + c_1 \cos(\theta - \theta_{la})$ where y is the cell's average firing frequency, b_0 is a baseline and c_1 is the gain in the cosine tuning on the difference between the load angle θ and the cell's preferred 'load axis' θ_{la}. For the simulation, we compare the cell's activation between a no-load condition and a condition with a load of $E_1 = 0.1$.

The rank-ordering of load sensitivity in the data is: phasic-MT < tonic < phasic-tonic. As shown in Figure 8, the rank ordering seen in the model for the corresponding cell types at the target holding time is similar: DVV, OPV < SFV, OFPV. The low THT load-sensitivity of OPV cells is due to the fact that the load compensation is progressively shifted during the movement to the SFV population. Because the OFPV sums inputs from OPV and SFV, it is largely indifferent to the shift in load from OPV to SFV during the movement. Consequently, its load sensitivity is nearly constant during the MT and THT.

The model proposes that in addition to summing the OPV and SFV signals, the OFPV stage also receives the IFV signal. This three-way summation scheme could lead to undesirable saturation of single cells under heavy loading conditions. This consideration combines with observations of a 'continuum' of phasic tonic cells (Kalaska *et al.*, 1989) to suggest a slightly different, less saturation-prone scheme that is otherwise computationally equivalent. Populations of pyramidal tract neurons (PTNs) in motor cortex exhibit recruitment as loads increase (Evarts *et al.*, 1983), with small cells (distinguished by long antidromic latency to spinal stimulation) recruited before large cells (of short antidromic latency). It is also known that small PTNs exhibit more tonic activity than the more transient large PTNs (Fromm *et al.*, 1984) and that a continuum exists between large transient cells and small tonic cells. These findings suggest the possibility of a distributed population of pyramidal tract neurons (OFPV cells) that receive different gradients of input from velocity error (IFV) and integrated position error (SFV), such that large, late recruited cells receive more IFV input than small cells, while the small cells receive more SFV input. This would help prevent saturation of OFPV cells during tasks requiring generation of large forces. Though beyond the scope of the present simulations, we predict that such a distributed population would exhibit phasic RT, phasic-tonic and tonic responses from large, medium and small PTNs respectively.

Control of the Response to External Forces

Due to GO signal gating, the model is capable of two different modes of response to external forces. When the GO signal is positive, the system resists external perturbations whether these are caused by loads or by external objects. When the GO signal is zero, the system passively submits to these forces. Figure 9 illustrates the difference between these responses. In the top row is shown the behavior with positive GO signal and in the bottom row the behavior with zero GO signal, in response to two different kinds of external forces.

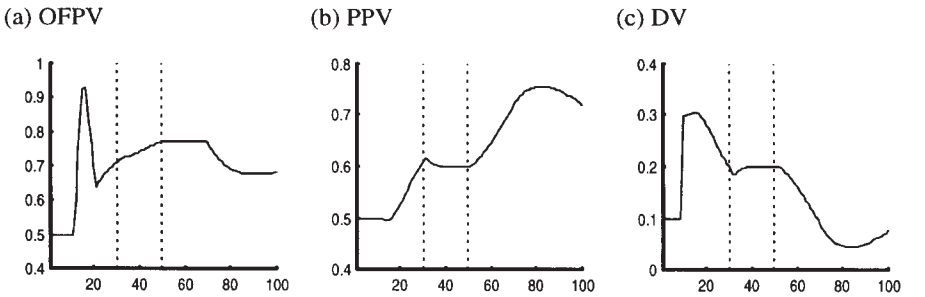

Figure 10. Simulation of model activities during a task involving exertion of forces against an obstacle. The vertical dashed lines indicate the time of the first contact with the obstacle and the time at which the obstacle yields. $g^{(0)} = 0.75$, $h = 0.1$, $\lambda_1 = 150$, $\tau = 0$.

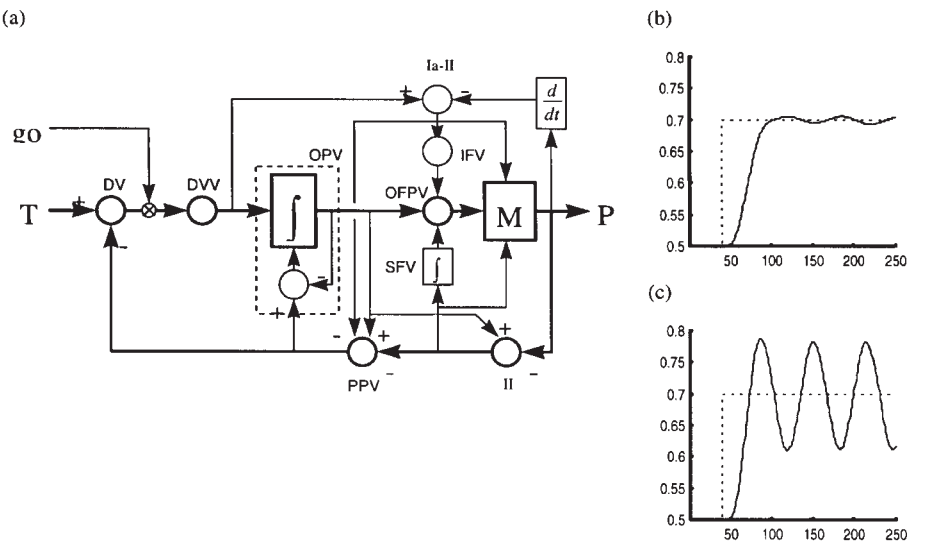

Figure 11. Comparison with PID control. (*a*) The model of Figure 1 represented with control theory notation. Again, the thick lines highlight the kinematic feedback control aspects of the system. (*b*) Position trace during a reaching movement made with the PPV–OPV pathway intact. (*c*) Reaching movement made without the PPV–OPV pathway ($\eta = 0$).

Simulations of Novel Experimental Tasks: Further Model Predictions

Because the functional scope of the model goes beyond the functional range probed in prior single-cell recording experiments, it generates testable hypotheses regarding cell responses during novel experimental paradigms. Predictions for one such paradigm are presented here.

Point-to-point Movements that Require Pushing through a Virtual Obstacle

A single-joint reaching movement is made to a specified target while the hand grasps a servo-controlled manipulandum. Shortly after movement initiation, on a random subset of trials, the manipulandum behaves as if it has encountered an obstacle that blocks movement toward the target, but then yields after a fixed level of force is exerted by the monkey in that direction. Reward is given only if the monkey exerts the required force vector and then continues its trajectory to the target. Meanwhile, recordings are taken from areas 4 and 5.

Qualitative predictions of the model for three cell types are shown in Figure 10. The activity of tonic cells in anterior area 5 (PPV) should remain unchanged during the time that the obstacle prevents movement. The activity of phasic cells in posterior area 5 (DV) should also remain unchanged during obstruction, and decay to baseline after the obstacle yields. Finally, during the contact time with the virtual obstacle, the population vector of phasic-tonic cells in area 4 (OFPV) should move past the value ordinarily associated with the position of the obstacle (as assessed on control trials) and toward the value associated with the target's position. The amount by which it will move past the obstacle should depend upon the level of force required to overcome the obstacle.

Comparison with PID Control.

Figure 11 represents the network model of Figure 1 with conventions familiar from control theory (Kuo, 1991). This comparison suggests that the network might be characterized as a trajectory generator in cascade with a PID (proportional-integral-derivative) controller. In particular, the spinal stretch reflex provides a component proportional to the position error, the SFV provides a component proportional to the integral of the position error, and the IFV provides a component proportional to the time derivative of the position error. Here the errors in question are those measured by the spindle subsystem, whose reference signals are provided by the OPV and DVV. Use of the DVV, or desired velocity, as input to gamma-dynamic MNs allows substitution of a direct measurement of velocity error for an otherwise necessary, but more noise-sensitive, neural differentiation. This direct measurement mechanism is reminiscent of the pursuit eye movement system's direct sensing of retinal 'slip'

(retinal image translation rate, the difference between eye velocity and object velocity), which is used as an error signal in that system (Lisberger *et al.*, 1981; Kawato and Gomi, 1992).

Equally important are the many ways that the design departs from standard PID control. Already noted was that the timing of the phasic RT pulse suggests a feedforward velocity error compensation, and the timing of some tonic cell updating suggests feedforward static load compensation (see also Crago *et al.*, 1976). However, the most significant departure is the simultaneously operating trajectory generator, which gradually changes the OPV in the direction of the TPV. A force-generating PID controller could in principle operate directly on a reference signal provided by the TPV. However, such a system would no longer exhibit the characteristics of voluntary movement, because movement would then be directly driven by external changes to the TPV. Because there is no gating and scaling within the PID-like part of the network, characteristics of voluntary movement such as the continuous control of speed, of halting and restarting would be lost. Also, when one TPV was abruptly replaced by another separated from the first by a large distance, a PID-only system would suddenly cease monitoring error relative to its current posture and relative to all postures intermediate between the initial and desired posture. Thus there would be no reflexive stabilization of the system at any intermediate point of the trajectory. Such a strategy would be disastrous for an animal moving loads (like its body) in a gravity field. The gravity load on a muscle is configuration dependent, so the load compensation needed at the end of the trajectory need have nothing to do with that needed to prevent a collapse at intermediate points along the trajectory (consider a quadruped raising itself off the ground). By specifying a continuous series of intermediate desired postures, the trajectory generator avoids this problem.

The trajectory generator is also distinguished by the time-varying gain provided by the GO signal, which contrasts with the constant gain used in conventional PID control. This change generates more symmetrical velocity profiles, and allows smaller peak accelerations, than are characteristic of standard PID control. Another notable property of the trajectory generator is created by the reciprocal connections between the OPV and the PPV stages. The significance of this feature is illustrated in Figure 11*b*,*c*, where two trajectories made under inertial load are shown. During the Figure 11*b* simulation, the circuit was intact, but in Figure 11*c* the circuit had been 'lesioned': there was no term corresponding to the signal carried by the pathway from the PPV to the OPV stage. The comparison reveals that the dynamics are much more favorable with the reciprocal pathway (Fig. 11*b*) than without it (Fig. 11*c*). The main reason is that the PPV to OPV projection greatly reduces what would otherwise be a significant overshoot of the OPV's normal value during the phase of the movement when the limb-plus-load is badly lagging the unperturbed trajectory. In short, this projection tends to prevent the system from using an atypical 'virtual trajectory' of the OPV stage as a solution to the inertial load problem, thus forcing any compensation into the IFV channel, which appears to involve feedforward action by the cerebellum. This division of labor is important because the OPV, unlike the IFV, projects to gamma motoneurons, and thus has the potential to mediate a transient positive feedback to the error signal, which would be progressively destabilizing with longer conduction and muscle-action delays. From another perspective, the PPV to OPV pathway serves to adjust the 'period' or half-cycle duration of the trajectory generator to the characteristics of the load. The OPV's tendency to track the PPV reduces velocity, at the cost of a modest prolongation of the point-to-point movement, but with the benefit of reducing the net forces required to accelerate and decelerate the larger load. In sum, the network's several departures from PID behavior create a kinematic planning circuit which is less oscillatory in the presence of load-related lags, which makes more modest demands for peak and total forces, and which affords reflex stabilization around all intermediate points of the trajectory.

Discussion

Cortical cells that are involved in voluntary reaching can be categorized into different cell types on many bases, including time of recruitment, mix of phasic and tonic components, response to perturbations, load-sensitivity, and tuning for position, direction and velocity. As the connectivity among sensory-motor areas has become clearer, it has become possible to tabulate (see Tables 1 and 2) physiological cell types and interactions that together strongly constrain the form of neural models. The good match of the proposed model between simulation and data are consistent with a number of conclusions. First, cortically controlled reaching movements can be adapted on-line to voluntary speed variations or imposed loading variations. Second, the production of movements with desirable kinematics can often be achieved, despite such variations, using kinesthetic feedback that corrects central representations of limb position. Third, kinesthetic feedback from the muscle spindles provides a kinematic error signal as long as gamma motoneurons are so activated that the intrafusal contraction matches the expected (desired) contraction of the extrafusal. Such a scheme tends to keep the spindle receptor in its optimal range by preventing unloading or excessive stretching, both of which compromise the quality of kinesthetic feedback. Treating the spindle signals as carriers of an error signal does not preclude a role for spindle signals in registering body configuration ('body image'). Fourth, because the kinesthetic subsystem judges in which directions forces must be generated to achieve kinematic goals, the kinesthetic system does not receive inputs from cells primarily responsible for generating directed compensatory forces. Thus gamma-MNs do not receive inputs from spindles. Also, neither area 5 position-related cells nor gamma motoneurons receive signals from those inertial and/or static load sensitive cells in area 4 that are interposed between the output cells of the central kinematic generator and the alpha-MNs. Fifth, there exists a voluntary gate between area 5 cells that compute the residual distance to target for a given arm and area 4 cells that compute desired movement velocity. Area 5 activity can hereby be decoupled from the immediate intention to act, and can serve a priming function. Priming allows preparation and deliberation. Thus, the model highlights a close mechanistic link between deliberation and volition. Although deliberation on the speed of movement is possible in the context of the model, this is not explored here. Sixth, variations in how the volitional gate is opened allow control of movement speed and trajectory shape. Breakdowns in the gating pathway lead to changes in movement speed and initiation while leaving movement direction invariant. Studies documenting pallido-nigral gating of voluntary eye movements (Hikosaka and Wurtz, 1985), skeletomotor bradykinesia following nigral lesions in Parkinson's disease and *N*-methyl-4-phenyl-1,2,3,6-tetrahydropyridine (MPTP) treatment (Doudet *et al.*, 1985), and pure speed effects of pallidal and thalamic stimulation (Mateer, 1978; Horak and Anderson, 1984b) suggest that final voluntary gating and

release of primed movements may be achieved via fronto-striato-pallido-thalamo-cortical pathways, which have terminations in a number of areas, including areas 4 and 6.

Omitted Cell Types and Implications for Analysis of Single-cell Data

The model does not treat a number of cortical cell types that are clearly related to preparation and execution of voluntary movements. These include primable cells in area 6 and area 4 (Alexander and Crutcher, 1990) and more frontal areas, 'reversal' cells in area 5 (Kalaska *et al.*, 1990), and various cell types in somatosensory and parietal cortex (Prud'homme and Kalaska, 1994). Some of these appear to contribute to functions, such as memory-based serial movements (SMA) or more complexly conditioned movements (lateral area 6), which fall outside the current scope of the model (Passingham, 1993). Others might be of more immediate relevance. For example, though there are many reports of poor primability of area 4 cells, some reports indicate reliable priming in motor cortex (Alexander and Crutcher, 1990). Generally, we expect to find that primable cells in precentral cortex will be found to be more rostral because all observers have reported strong primability in such areas as the dorsal aspect of the lateral premotor cortex (Alexander and Crutcher, 1990; Kalaska and Crammond, 1995). Though the model in its lumped version does not include primable area 4 cells, it is compatible with them. For example, such cells may be indicative of a coordinate transformation between a more spatial parietal DV and a more muscle-related DV in area 4. In addition, primable cells in area 4 may play a role in stiffening the limb in preparation for movement. There is a model-independent constraint on whether any motor cortical cell with monosynaptic contacts on motoneurons can be primed: because there is no intermediate neuron at which gating could occur, to prime a population of corticomotoneuronal area 4 cells would pre-activate the movement, unless the area 4 projection was restricted to high-threshold motoneurons. One exception could be the co-contraction cells reported to exist in area 4 by Humphrey and Reed (1983), which may be used in increasing joint stiffness as mentioned above.

Cell properties in cortex do not always neatly partition into the distinct functional classes outlined by the model, but rather may form a more complex continuum of which the modeled types are lumped representations. Other cell types may be produced from different combinations of SFV, IFV and OPV signals and may emerge from a distributed OFPV population as described above in the context of load-compensation.

By specifying, at least partially, distinct computational roles for the diverse cell types within area 4, the model raises serious questions about the general appropriateness of methods that average single-cell recordings across populations of task-related neurons without regard to cell type. The results reported in Kalaska and Drew (1993) support this perspective by showing that novel insights may be gained by averaging within but not across pools of physiologically identified cell-types.

From this perspective, an affirmative reply can be developed to the question of Fetz (1992) as to whether movement parameters are recognizably coded in the activity of single neurons. Properties of model cells with clear functional roles co-vary with cell responses observed in the cortex. Many of the puzzling properties of kinematic and kinetic sensitivities in areas 4 and 5 mentioned earlier hereby become explicable. Planning the task is best done using kinematic variables such as those observed in area 5 and in some cells in area 4. Superimposed upon this kinematic planning circuit are several compensatory circuits which assemble command components needed to reduce errors due to static and inertial loads. As Kalaska and Crammond (1995) have noted, kinematic and kinetic variables are inextricably linked by the Newtonian laws of motion. The model reflects this linkage in a functionally explicit way.

Relationship to other Proposals Regarding Movement Control and Proprioception

Prior models aimed at explaining properties of cortical cells focus primarily upon the directional tuning observed in these cells (Burnod *et al.*, 1992; Berthier *et al.*, 1993; Georgopoulos *et al.*, 1993; Houk *et al.*, 1993; Kettner *et al.*, 1993; Lukashin and Georgopoulos, 1993; Redish and Touretzky, 1994), usually in the context of sensorimotor transformations. While these models focus on population statistics and simplify temporal dynamics, the present model simplifies population statistics to elaborate temporal dynamics. It is thus compatible with the results of these other models regarding issues it does not address. For example, the model of Redish and Touretzky (1994) reaches conclusions similar to ours concerning the functional significance of the load-sensitivity differences between areas 4 and 5.

The model's thesis that movement control involves a gradually shifting positional command shares features with recent equilibrium point formulations (see Bizzi *et al.*, 1992 for a review). In contrast to most other equilibrium point discussions, however, we do not suggest that limb dynamics can be ignored, and explicitly include mechanisms for static and inertial load compensation which are superimposed upon the kinematic command. Also, we propose that trajectory generation is guided in part by feedback information. This allows the model to reproduce the endpoint errors observed during human pointing movements performed in a Coriolis force-field (Lackner and DiZio, 1994), as demonstrated in a companion report (Cisek *et al.*, 1996)

The proposal that proprioception is based on feedback correction of an efference copy is shared by the theory of Burgess *et al.* (1995) and by the lambda hypothesis (Feldman and Latash, 1982; Feldman, 1986). The desired effort command (E-DAP) of Burgess *et al.* (1995) is guided by comparisons between desired visual and kinesthetic profiles and the feedback from various peripheral receptors, including spindles. In the lambda model, the brain estimates joint angle by starting with a corollary discharge of a motor command and adding to it a correction factor based on muscle stiffness and load-dependent deviations from expected torque. How the two factors needed to compute the correction factor could be known was not specified. By its dependence on torque sensing, that proposal implicates Golgi tendon organs, rather than spindles, as principal contributors to position sense. As shown in a complementary report of simulations modeling vibration-induced proprioceptive illusions and related effects (Cisek *et al.*, 1996), the model proposed here is consistent with experimental data indicating that the spindle feedback is dominant in limb proprioception (Goodwin *et al.*, 1972; Clark *et al.*, 1979).

Notes

D.B. supported by the Office of Naval Research (ONR N00014-92-J-1309, ONR N00014-93-1-1364 and ONR N00014-95-1-0409). P.C. supported in part by the Defense Advanced Research Projects Agency (ONR N00014-92-J-4015), the National Science Foundation (NSF IRI-90-24877 and NSF IRI-90-00530), the Office of Naval Research (ONR N00014-93-1-1364 and ONR N00014-95-1-0409), Fond pour la formation de Chercheurs et l'Aide à la Recherche (FCAR 124-82-058-000), and the

Medical Research Council (MRC 124-29-058-490). Now at Centre de Recherche en Sciences Neurologiques, Department de Physiologie, Université de Montreal. S.G. supported in part by the Office of Naval Research (ONR N00014-92-J-1309 and ONR N00014-95-1-0409).

Address correspondence to Daniel Bullock or Stephen Grossberg, Department of Cognitive and Neural Systems, Boston University, 677 Beacon Street, Boston, MA 02215, USA. Email: danb@cns.bu.edu, steve@cns.bu.edu.

References

Alexander GE, Crutcher MD (1990) Preparation for movement: neural representations of intended direction in three motor areas of the monkey. J Neurophysiol 64:133–150.

Anderson RA (1987) Inferior parietal lobule function in spatial perception and visuomotor integration. In: Handbook of physiology, Section 1: The nervous system, Vol. V: Higher functions of the brain, Part 2 (Plum F, Mountcastle VB, Geiger SR eds), pp. 483–518. Bethesda, MD: American Physiological Society.

Berthier NE, Singh SP, Barto AG, Houk JC (1993) Distributed representations of limb motor programs in arrays of adjustable pattern generators. J Cognit Neurosci 5:56–78.

Bizzi E, Accornero N, Chapple W, and Hogan N (1984) Posture control and trajectory formation during arm movement. J Neurosci 4:2738–2744.

Bizzi E, Hogan N, Mussa-Ivaldi FA, Giszter SF (1992) Does the nervous system use equilibrium-point control to guide single and multiple joint movements? Behav Brain Sci 15:603–613.

Brooks VB (1986) The neural basis of motor control. New York: Oxford University Press.

Bullock D, Contreras-Vidal JL (1993) How spinal neural networks reduce discrepancies between motor intention and motor realization. In: Variability and motor control (Newell KM, Corcos DM, eds), pp. 183–221. Champaign, IL: Human Kinetics Press.

Bullock D, Grossberg S (1988) Neural dynamics of planned arm movements: emergent invariants and speed-accuracy properties during trajectory formation. Psychol Rev 95:49–90.

Bullock D, Grossberg S (1989) VITE and FLETE: neural modules for trajectory formation and postural control. In: Volitional action (Hershberger WA, ed.), pp. 253–297. Amsterdam: North-Holland/Elsevier.

Bullock D, Grossberg S (1990) Spinal network computations enable independent control of muscle length and joint compliance. In: Advanced neural computers (Eckmiller R, ed.), pp. 349–356. Amsterdam: Elsevier.

Bullock D, Grossberg S (1991) Adaptive neural networks for control of movement trajectories invariant under speed and force rescaling. Hum Move Sci 10:1–51.

Bullock D, Grossberg S, Guenther FH (1993) A self-organizing neural model of motor equivalent reaching and tool use by a multijoint arm. J Cognit Neurosci 5:408–435.

Burbaud P, Doegle C, Gross C, Bioulac B (1991) A quantitative study of neuronal discharge in areas 5, 2, and 4 of the monkey during fast arm movements. J Neurophysiol 66:429–443.

Burgess PR, Cooper TA, Gottlieb GL, Latash ML (1995) The sense of effort and two models of single-joint motor control. Somatosens Mot Res 12:343–358.

Burnod Y, Grandguillaume P, Otto I, Ferraina S, Johnson PB, Caminiti R (1992) Visuomotor transformations underlying arm movements toward visual targets: a neural network model of cerebral cortical operations. J Neurosci 12:1435–1453.

Caminiti R, Johnson PB, Galli C, Ferraina S, Burnod Y (1991) Making arm movements within different parts of space: the premotor and motor cortical representations of a coordinate system for reaching to visual targets. J Neurosci 11:1182–1197.

Chapman CE, Spidalieri G, Lamarre Y (1984) Discharge properties of area 5 neurones during arm movements triggered by sensory stimuli in the monkey. Brain Res 309:63–77.

Cheney PD, Fetz EE (1980) Functional classes of primate corticomotoneuronal cells and their relation to active force. J Neurophysiol 44:773–791.

Cheney PD, Fetz EE (1984) Corticomotoneuronal cells contribute to long-latency stretch reflexes in the rhesus monkey. J Physiol 349:249–272.

Cisek P, Grossberg S, Bullock D (1996) A cortico-spinal model of reaching and proprioception under multiple task constraints. Boston University Technical Report CAS/CNS TR-96–035. J Cognit Neurosci (in press).

Clark FJ, Horch KW, Bach SM, Larson GF (1979) Contributions of cutaneous and joint receptors to static knee-position sense in man. J Neurophysiol 42:877–888.

Contreras-Vidal JL, Grossberg S, Bullock D (1997) A neural model of cerebellar learning for arm movement control: cortico-spino-cerebellar dynamics. Learn Mem 3:475–502.

Crago PE, Houk JC, Hasan Z (1976) Regulatory actions of human stretch reflex. J Neurophysiol 39:925–935.

Crammond DJ, Kalaska JF (1989) Neuronal activity in primate parietal cortex area 5 varies with intended movement direction during an instructed-delay period. Exp Brain Res 76:458–462.

Crutcher MD, Alexander GE (1990) Movement-related neuronal activity selectively coding either direction or muscle pattern in three motor areas of the monkey. J Neurophysiol 64:151–163.

Doudet D, Gross C, Lebrun-Grandie P, Bioulac B (1985) MPTP primate model of Parkinson's disease: a mechanographic and electromyographic study. Brain Res 335:194–199.

Dum RP, Strick PL (1990) Premotor areas: nodal points for parallel efferent systems involved in the central control of movement. In: Motor control: concepts and issues (Humphrey DR, Freund DR, eds), pp. 383–397. London: Wiley.

Evarts EV (1968) Relation of pyramidal tract activity to force exerted during voluntary movement. J Neurophysiol 31:14–27.

Evarts EV (1973) Motor cortex reflexes associated with learned movement. Science 179:501–503.

Evarts EV (1974) Precentral and postcentral cortical activity in association with visually triggered movement. J Neurophysiol 37:373–381.

Evarts EV, Fromm C, Kröller J, Jennings VA (1983) Motor cortex control of finely graded forces. J Neurophysiol 49:1199–1215.

Evarts EV, Tanji J (1974) Gating of motor cortex reflexes by prior instruction. Brain Res 71:479–494.

Feldman AG (1986) Once more on the equilibrium-point hypothesis (lambda model) for motor control. J Mot Behav 18:17–54.

Feldman AG, Latash ML (1982) Interaction of afferent and efferent signals underlying joint position sense: empirical and theoretical approaches. J Mot Behav 14:174–193.

Fetz EE (1992) Are movement parameters recognizably coded in the activity of single neurons? Behav Brain Sci 15:679–690.

Fiala JC, Grossberg S, Bullock D (1996) Metabotropic glutamate receptor activation in cerebellar Purkinje cells as substrate for adaptive timing of the classically conditioned eye-blink response. J Neurosci 16:3760–3774.

Fromm C, Evarts EV (1982) Pyramidal tract neurons in somatosensory cortex: central and peripheral inputs during voluntary movement. Brain Res 238:186–191.

Fromm C, Wise SP, Evarts EV (1984) Sensory response properties of pyramidal tract neurons in the precentral motor cortex and postcentral gyrus of the rhesus monkey. Exp Brain Res 54:177–185.

Fu Q-G, Suarez JI, Ebner TJ (1993) Neuronal specification of direction and distance during reaching movements in the superior precentral premotor area and primary motor cortex of monkeys. J Neurophysiol 70:2097–2116.

Gachoud JP, Mounoud P, Havert P, Viviani P (1983) Motor strategies in lifting movements: a comparison of adult and child performance. J Mot Behav 15:202–216.

Georgopoulos AP (1995) Current issues in directional motor control. Trends Neurosci 18:506–510.

Georgopoulos AP, Caminiti R, Kalaska JF (1984) Static spatial effects in motor cortex and area 5: quantitative relations in a two-dimensional space. Exp Brain Res 54:446–454.

Georgopoulos AP, Kalaska JF, Caminiti R, Massey JT (1982) On the relations between the direction of two-dimensional arm movements and cell discharge in primate motor cortex. J Neurosci 2:1527–1537.

Georgopoulos AP, Taira M, Lukashin AV (1993) Cognitive neurophysiology of the motor cortex. Science 260:47–52.

Goodwin GM, McCloskey DI, Matthews PBC. (1972) The contribution of muscle afferents to kinæsthesia shown by vibration induced illusions of movement and by the effects of paralysing joint afferents. Brain 95:705–748.

Hikosaka O, Wurtz RH (1985) Modification of saccadic eye movements by GABA-related substances. II. Effects of muscimol in the monkey substantia nigra pars reticulata. J Neurophysiol 53:282–308.

Horak FB, Anderson ME (1984a). Influence of globus pallidus on arm

movements in monkeys. I. Effects of kainic acid-induced lesions. J Neurophysiol 52:290–304.
Horak FB, Anderson ME (1984b). Influence of globus pallidus on arm movements in monkeys. II. Effects of stimulations. J Neurophysiol 52:305–322.
Houk JC, Keifer J, Barto AG (1993) Distributed motor commands in the limb premotor network. Trends Neurosci 16:27–33.
Humphrey DR, Reed DJ (1983) Seperate cortical systems for control of joint movement and joint stiffness: reciprocal activations and coactivation of antagonist muscles. In: Motor control mechanisms in health and disease (Desmedt JE, ed.), pp. 347–372. New York: Raven Press.
Ito M (1984) The cerebellum and neural control. New York: Raven Press.
Jennings VA, Lamour Y, Solis H, Fromm C (1983) Somatosensory cortex activity related to position and force. J Neurophysiol 48:1216–1229.
Johnson PB, Ferraina S, Caminiti R (1993) Cortical networks for visual reaching. Exp Brain Res 97:361–365.
Jones EG, Coulter JD, Hendry HC (1978) Intracortical connectivity of achitectonic fields in the somatic sensory, motor and parietal cortex of monkeys. J Comp Neurol 181:291–348.
Kalaska JF (1996) Reaching movements: implications of connectionist models. In: Handbook of brain theory and neural networks (Arbib M, ed.), pp. 788–793. Cambridge, MA: MIT Press.
Kalaska JF, Crammond DJ (1995) Deciding not to GO: neuronal correlates of response selection in a GO/NOGO task in primate premotor and parietal cortex. Cereb Cortex 5:410–428.
Kalaska JF, Drew T (1993) Motor cortex and visuomotor behavior. Exercise Sports Sci Rev 21:397–436.
Kalaska JF, Hyde ML (1985) Area 4 and area 5: differences between the load direction-dependent discharge variability of cells during active postural fixation. Exp Brain Res 59:197–202.
Kalaska JF, Cohen DAD, Hyde ML, Prud'homme MJ (1989) A comparison of movement direction-related versus load direction-related activity in primate motor cortex, using a two-dimensional reaching task. J Neurosci 9:2080–2102.
Kalaska JF, Cohen DAD, Prud'homme MJ, Hyde ML (1990) Parietal area 5 neuronal activity encodes movement kinematics, not movement dynamics. Exp Brain Res 80:351–364.
Kato M, Kimura M (1992) Effects of reversible blockade of basal ganglia on a voluntary arm movement. J Neurophysiol 65:1516–1534.
Kawato M, Gomi H (1992) The cerebellum and VOR/OKR learning models. Trends Neurosci 15:445–453.
Kettner RE, Marcario J, Port N (1993) A neural network model of cortical activity during reaching. J Cognit Neurosci 5:14–33.
Kettner RE, Schwartz AB, Georgopoulos AP (1988) Primate motor cortex and free arm movements to visual targets in three-dimensional space. III. Positional gradients and population coding of movement direction from various movement origins. J Neurosci 8:2938–2947.
Kuffler SW, Hunt CC (1952) The mammalian small-nerve fibers: a system for efferent nervous regulation of muscle spindle discharge. In: Patterns of organization in the central nervous system (Bard P, ed.), pp. 24–47. Baltimore, MD: Williams and Wilkins.
Kuo BC (1991) Automatic control systems. Englewood Cliffs, NJ: Prentice Hall.
Lackner JR, DiZio P (1994) Rapid adaptation to Coriolis force perturbations of arm trajectory. J Neurophysiol 72:299–313.
Lacquaniti F, Guigon E, Bianchi L, Ferraina S, Caminiti R (1995) Representing spatial information for limb movement: role of area 5 in the monkey. Cereb Cortex 5:391–409.
Lestienne F (1979) Effects of inertial loads and velocity on the braking process of voluntary limb movements. Exp Brain Res 35:407–418.
Lisberger SG, Evinger C, Johanson GW, Fuchs AF (1981) Relationship between eye acceleration and retinal image velocity during foveal smooth pursuit in man and monkey. J Neurophysiol 46:229–249.
Lukashin AV, Georgopoulos AP (1993) A dynamical neural network model for motor cortical activity during movement: population coding of movement trajectories. Biol Cybernet 69:517–524.
Mateer C (1978) Asymmetric effects of thalamic stimulation on rate of speech. Neuropsychologia 16:497–499.
Matthews PBC (1988) Proprioceptors and their contribution to somatosensory mapping: complex messages require complex processing. Can J Physiol Pharmacol 66:430–438.
McCloskey DI, Cross MJ, Honner R, Potter EK (1983) Sensory effects of pulling or vibrating exposed tendons in man. Brain 106:21–37.
Mussa-Ivaldi FA (1988) Do neurons in the motor cortex encode movement direction? An alternate hypothesis. Neurosci Lett 91:106–111.
Oscarsson O, Rosen I (1963) Projection to cerebral cortex of large muscle-spindle afferents in forelimb nerves of the cat. J Physiol 169:924–945.
Pandya DN, Kuypers HGJ.M. (1969) Cortico-cortical connections in the rhesus monkey. Brain Res 13:13–36.
Passingham RE (1993) The frontal lobes and voluntary action. Oxford: Oxford University Press.
Phillips CG, Powell TPS, Wiesendanger M (1971) Projection from low-threshold muscle afferents of hand and forearm to area 3a of baboon's cortex. J Physiol 217:419–446.
Prud'homme MJ, Kalaska JF (1994) Proprioceptive activity in primate primary somatosensory cortex during active arm reaching movements. J Neurophysiol 72:2280–2301.
Redish DA, Touretzky DS (1994) The reaching task: evidence for vector arithmetic in the motor system? Biol Cybernet 71:307–317.
Riehle A, MacKay WA, Requin J (1994) Are extent and force independent movement parameters? Preparation- and movement-related neuronal activity in the monkey cortex. Exp Brain Res 99:56–74.
Robinson CJ, Burton H (1980) Organization of somatosensory receptive fields in cortical areas 7b, retroinsular postauditory and granular insula of *M. fascicularis*. J Comp Neurol 192:69–92.
Sanger TD (1994) Theoretical considerations for the analysis of population coding in motor cortex. Neural Comput 6:29–37.
Schwartz AB (1992) Motor cortical activity during drawing movements: single unit activity during sinusoid tracing. J Neurophysiol 68:528–541.
Schwartz AB (1993) Motor cortical activity during drawing movements: population representation during sinusoid tracing. J Neurophysiol 70:28–36.
Scott SH, Kalaska JF (1995) Changes in motor cortex activity during reaching movements with similar hand paths but different arm postures. J Neurophysiol 73:2563–2567.
Strick PL, and Kim CC (1978) Input to primate motor cortex from posterior parietal cortex (area 5). I. Demonstration by retrograde transport. Brain Res 157:325–330.
Vallbo ÅB (1981) Basic patterns of muscle spindle discharge in man. In: Muscle receptors and movement (Taylor A, Prochazka A, eds), pp. 263–275. London: Macmillan.
Vilis T, Hore J (1980) Central neural mechanisms contributing to cerebellar tremor produced by perturbations. J Neurophysiol 43:279–291.
Zarzecki P, Strick PL, Asanuma H (1978) Input to primate motor cortex from posterior parietal cortex (area 5). II. Identification by antidromic activation. Brain Res 157:331–335.

Appendix: Model Parameters

Except where noted, all the simulations above use the following parameter settings: $I = 200$, $V = 10$, $\nu = 0.15$, $B^{(r)} = 0.1$, $B^{(u)} = 0.01$, $\Theta = 0.5$, $\theta = 0.5$, $\phi = 1$, $\eta = 0.7$, $\rho = 0.04$, $\lambda_i = 10$, $\Lambda = 0.001$, $\delta = 0.1$, $C = 25$, $\varepsilon = 0.05$, $\psi = 4$, $h = 0.01$, $\tau = 3$. In the simulations shown in Figures 3, 4 and 10, τ is reduced to zero and λ_1 increased to approximate the feedforward dynamics compensation which generates the large launching pulse seen in the OFPV activation profile.